SOFTENING THE HABITATS
SUSTAINABLE INNOVATION IN MINIMAL MASS STRUCTURES AND LIGHTWEIGHT ARCHITECTURES

Proceedings of the TensiNet Symposium 2019
Softening the habitats | 3-5 June 2019, Politecnico di Milano, Milan, Italy
Alessandra Zanelli, Carol Monticelli, Marijke Mollaert, Bernd Stimpfle (Eds.)

Thermal performance of pneumatic cushions: an experimental evaluation

Andrea ALONGI*[a], Adriana ANGELOTTI*[a], Alessandro RIZZO[b], Alessandra ZANELLI[ac]

*Politecnico di Milano, Energy Department,
v. Lambruschini 4A, Milano 20156, Italy,
adriana.angelotti@polimi.it
[a]Textiles Hub, Politecnico di Milano, v. Ponzio 33, Milano 20133, Italy
[b]Canobbio textile engineering srl, Strada Sgarbazzolo, Castelnuovo Scrivia (AL) 15053, Italy
[c]Politecnico di Milano, ABC Department, v. Bonardi 3, Milano 21033, Italy

Abstract

In the recent past coated textiles and membrane structures have been increasingly implemented in architecture as either temporary or permanent external building envelopes. Double or multiple layer pneumatic cushions are frequently adopted. Therefore, one of their tasks is to guarantee suitable thermal conditions for the enclosed environment and/or limit HVAC energy consumption. The key thermal-physical parameter is then the cushion thermal resistance, which is usually assessed through simple calculations based on the assumption that cavities are approximated as rectangular enclosures. However, the impact of the actual shape of the cushions on the heat transfer has not been clarified yet. In this work, the thermal resistance of two cushions is experimentally assessed using a double chamber thermal setup. More precisely, two (double and triple layer) small vertical samples (1.1 m x 1.1 m) are exposed to a 25 °C steady-state temperature difference, to replicate Milan winter design conditions. Their exterior surfaces are divided in thermally homogeneous sub-surfaces of various sizes and temperatures are locally sampled on every sub-surface of both skins, along with the heat flux density on one side. Data are collected every 5 seconds for a time span of 12 h, in order to verify the steady-state assumption, and the average values for both temperatures and heat flux in every subsection are calculated. These data are then area-weighted and used to calculate the overall thermal resistance for each sample investigated, which are then compared with various correlations from literature.

Keywords: pneumatic cushion, thermal resistance, energy performance, measurement, heat flow, air gap, natural convection, multi-layered membrane skin.

DOI: 10.30448/ts2019.3245.02

Peer-review under responsibility of the TensiNet Association

1. Introduction

In the field of membranes structures, made of coated textiles or Fluor-polymeric foils, the pneumatic cushions are widely used with a variety of multilayered solutions, composed of 2 up to 5 layers, where the resulting air gaps are inflated to an extra-pressure of 200-300 Pa up to 600-900 Pa. Cushions can be also shaped with a quite high freedom by architects, while the manufacture optimization suggests adopting rectangular shapes, with a span of 3 meters and an almost infinite development in the other direction (Gomez-Gonzalez et al., 2011; Le Cuyer, 2008) .

The thermal transmittance of the cushion (i.e. the *U*-value), together with the solar gain factor (i.e. *g*-value), is the fundamental thermal-physical property for evaluating the energy behavior of the textile envelope (Afrin et al. 2015), as in the dynamic simulations of the pressostatic sports halls analyzed in (Suo et al. 2015). The cushion thermal transmittance depends on the heat flow direction (horizontal, upwards or downwards) and on the number of layers, which determines the number of air gaps. According to (Knippers et al., 2010), both CEN EN ISO 6946 and CEN EN 673 can be used to estimate the center-of-the cushion thermal transmittance in a roughly similar way, although no calculation method is able to catch the non-steady state heat transfer mechanism connected to natural convection inside the air cavities. Following the standards calculations, for the horizontal heat flow direction, passing from a double layer cushion to a triple layer allows to reduce the wintertime *U*-value from about 3 W/(m^{2}K) to about 2 W/(m^{2}K).

The center-of-the cushion *U*-value, representing the portion where the layers are almost plane and parallel, does not take into account the impact of the curved shape of the cushion. Mainini et al. (Mainini et al., 2011) measure the thermal conductance of a double layer panel (dimensions: 1050 x 1140 mm) realized with two ETFE membranes, finding that C = 5.158 W/(m^{2}K) and U = 2.748 W/(m^{2}K). However, the two layers are parallel to each other and tensioned on an aluminum frame with no thermal break, therefore the effects of the typical curvature of the cushion are not considered. In turn in (Antretter et al., 2008) 2D CFD simulations on a large size double layer ETFE cushion with realistic curvature are performed, with the aim to study the flow patterns inside the cavity. For inclined cushions, one big roll is found with secondary flows in the upper and lower edges. For the horizontal cushion with heat flow upwards, several eddies are found, determining a good mixing in the cavity, a part from the edges.

Therefore further efforts are necessary to understand the heat transfer across cushions, including natural convection in the curved cavities, and then evaluate U-values more accurately than with present parallel planes assumptions.

2. Materials and Methods

This paper deals with a series of experimental tests performed on two pneumatic cushion samples of small size, namely a double layer and a triple layer with vertical orientation, in a laboratory apparatus. Collected data are processed to derive the thermal resistance and the thermal transmittance of each sample. The measured energy performances of the two cushions are then compared with each other. In the end experimental outcomes are compared to values obtained using literature correlations for free convection in vertical cavities.

2.1. The experimental setup

The experimental phase of this work consists of the evaluation of the cushion thermal resistance using a laboratory rig called Dual Air Vented Thermal Box (DAVTB), developed at the Building Physics Laboratory of the Energy Department of Politecnico di Milano. This setup is designed to test building envelope technologies under user-defined thermal boundary conditions (both in steady and unsteady state) and, if needed, to force an airflow through permeable components such as Breathing Walls. For the purpose of this study, the air flow loop is not used. A detailed description of the apparatus can be found in (Alongi et al. 2017).

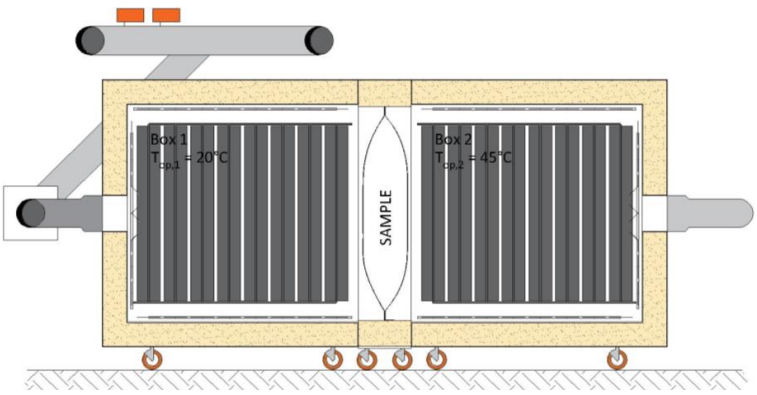

Figure 1: vertical section of the DAVTB apparatus. The radiant panels are visible both in Box 1 (left) and in Box 2 (right). The operative conditions adopted in this work are also reported, along with the cross section of one of the two samples experimentally investigated.

The DAVTB facility (Figure 1) consists of two insulated chambers (1.5 m x 1.5 m x 1.29 m each) divided by the sample and connected by the air recirculation system, used to generate an airflow through the sample, if needed. The operative temperature is set separately in each chamber, by means of a dedicated hydronic system providing both heating and cooling through radiant panels inside the boxes. The range of operative conditions achievable is between 15°C and 50°C. The sample is accommodated in a 1.5 m x 1.5 m metal frame interposed between the chambers and provided with thermal insulation, in order to minimize any edge effect. The

apparatus is supplied with two different frames: one is used to test regular 1 m x 1 m building walls with a maximum thickness of 30 cm, while the other one is dedicated exclusively to test 1.1 m x 1.1 m pneumatic cushions samples as in the present study. The measurement and control system in the DAVTB apparatus is based on an Agilent 34980A multifunctional switch unit, remotely controlled through a LabVIEW algorithm. As far as temperature measurements are concerned, they are sampled in various points of the hydraulic plant and in various locations inside each chamber, using T-type calibrated thermocouples (TC). A globe thermometer is installed in the geometrical center of each chamber to measure the operative temperature.

The thermal resistance of the cushion is measured through the heat flow and surface temperatures method, as in (GOST 26602.1-99). Therefore, 32 thermocouples and 16 heat flux meters (HFM) are installed to map temperature and heat flux density distribution on the sample surfaces. The HFMs are 5 gSKIN®-XM 26 9C (sensing dimensions 4.4 mm x 4.4 mm) and 11 gSKIN®-XI 26 9C (sensing dimensions 18.0 mm x 18.0 mm), with a ±3 % calibration accuracy according to the manufacturer GreenTeg.

In order to experimentally assess the thermal resistance of the two cushion samples, a constant operative temperature difference across the sample has been set, reproducing equal the design winter condition in Milan i.e. $\Delta T = 25$ °C. Considering the operative temperature range achievable in the apparatus such temperature difference has been established by setting 20 °C in Box 1 and 45 °C in Box 2. Environmental data (i.e. operative temperature in each chamber) and surface data (temperature and heat flux density) have been collected every 5 s for a time period of at least 12 h, in order to obtain a stable set of data that could confirm the steady-state hypothesis.

2.2. The samples

As already mentioned, the main core of this work is based on the experimental evaluation of the thermal resistance of two pneumatic cushions samples, like the one shown in Figure 2 (cross section visible in Figure 1). Double and triple layer configurations have been investigated, i.e. SAMPLE01 and SAMPLE02 respectively, both based on PVC coated polyester fabrics with grammage of 700 g/m^2 and 900 g/m^2, to replicate the inner and the outer surfaces of a real cushion. Thermal emissivity of both layers has been found equal to 0.85 through FTIR spectrophotometry measurements. Both cushions are kept inflated at an internal extra-pressure of 300 Pa using an intermittent air compressor.

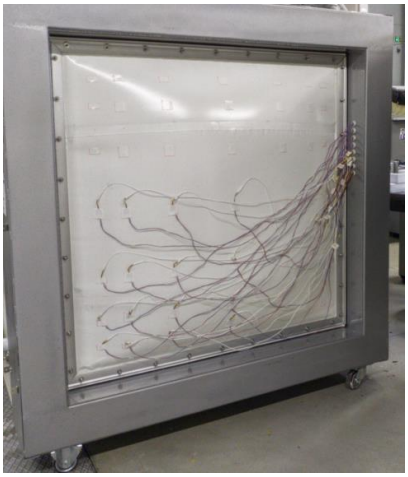

Figure 2: picture of the inflated SAMPLE01 (surface facing Box 2). Thermocouples and heat flux meters location is also visible.

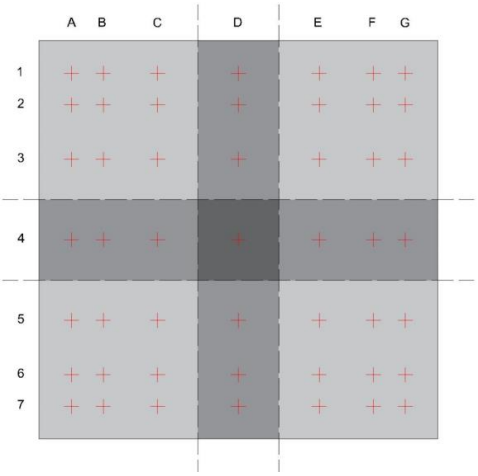

Figure 3: location on a general sample surface of the probing points, used as a reference for the mapping procedure of temperature and heat flux density. Overlapping areas are also visible.

For both cushions analyzed, the section is double-ogive shaped with a flatter region in the central section and steep tapering toward the edges. Due to this feature, temperature and heat flux density are expected to vary significantly throughout the surfaces. For this reason, the surfaces of the samples have been divided into 49 portions, with decreasing dimensions going from the center toward the edges (Figure 3). Surface temperatures and heat flows have been measured in the centers of each portion, indicated by the red crosses in Figure 3. Since the measured thermal emissivity of the heat flow meters is equal to 0.65, they are not matched in emissivity with the cushion materials. Therefore, HFMs have been covered with dedicated patches of the same textile material used to produce the cushions, to guarantee that they are subjected to the same radiative conditions of the investigated sample.

As it is possible to infer from Figure 3, the available amount of probes is not enough to cover the overall area in a single test. Therefore, the testing procedure applied to each cushion has been divided into four phases, in which temperatures and heat flux densities are measured on corresponding 4 rows-by-4 rows portions of the surfaces, as exemplified in Figure 2:

- phase 1 - from A1 to D4 on the Box 1 side and from D1 to G4 on the Box 2 side;
- phase 2 - from D1 to G4 on the Box 1 side and from A1 to D4 on the Box 2 side;
- phase 3 - from D4 to G7 on the Box 1 side and from A4 to D7 on the Box 2 side;
- phase 4 - from A4 to D7 on the Box 1 side and from D4 to G7 on the Box 2 side.

In this way, both the surfaces are covered completely, with data collected twice on column D and row 4 on both sides and four times on the D4 point. This redundancy allows to verify that

the same surface conditions have been achieved in different phases of the test, and thus all the collected data are coherent and can be treated as if they were gathered in a single test.

2.3. The data processing procedure

The most relevant data collected during every test are:

- the operative temperature $T_{op,1}$ for Box 1 and $T_{op,2}$ for Box 2;
- the surface temperature $T_{i,j,k}$ on each mapping point of both the sample surfaces, where, according to Figure 3, i represents the column (from A to G), j represents the row (from 1 to 7) and k represents the side of the sample (1 for the surface facing Box 1, 2 for the one facing Box 2);
- the heat flux density $\varphi_{i,j}$ on each mapping point of the surface facing Box 2.

Once steady state condition has been reached in a phase of the test, for every quantity mentioned above the time average is calculated. Those quantities that have been measured in more than one phase of the test have then been further averaged over the phases.

Subsequently the area weighted averages of surface temperatures and heat fluxes have been calculated using the following equations:

$$\overline{T}_{s,k} = \frac{\sum_{i=A}^{G}\sum_{j=1}^{7} A_{i,j}T_{i,j,k}}{\sum_{i=A}^{G}\sum_{j=1}^{7} A_{i,j}} \text{ (average surface temperature toward Box } k\text{)} \quad (1)$$

$$\overline{\varphi} = \frac{\sum_{i=A}^{G}\sum_{j=1}^{7} A_{i,j} \cdot \varphi_{i,j}}{\sum_{i=A}^{G}\sum_{j=1}^{7} A_{i,j}} \text{ (average heat flux density toward Box 2)} \quad (2)$$

where $A_{i,j}$ is the area surrounding the i,j mapping location on the sample surface. This comes from the hypothesis of thermal homogeneity over a given i,j area, and allows to mitigate any edge effect or singularity. The overall experimental thermal resistance of the cushion is then calculated as follows:

$$R_{\exp} = \frac{\overline{T}_{s,2} - \overline{T}_{s,1}}{\overline{\varphi}} \quad (3)$$

The experimental thermal transmittance, that includes the effects of the surface heat transfer coefficient in the apparatus, is evaluated from the average values of operative temperatures and the average heat flux density calculated through (2), i.e.:

$$U_{\exp} = \frac{\bar{\varphi}}{T_{op,2} - T_{op,1}} \tag{4}$$

At the same time, using the conventional values for the surface heat transfer coefficients (h_{ext} and h_{int} equal to 25 W/(m^{2}K) and 7.7 W/(m^{2}K) respectively), the standard thermal transmittance is calculated as:

$$U_{std} = \frac{1}{\frac{1}{h_{ext}} + R_{\exp} + \frac{1}{h_{\text{int}}}} \tag{5}$$

The experimental thermal resistances R_{exp} for the two cushions derived through Eq. (3) are then compared to the thermal resistances in vertical cavities (i.e. parallel surfaces) calculated using natural convection correlations from literature, which are generally used to assess the overall performance of cushions. Neglecting the conductive resistance of the very thin fabric layers, the calculated thermal resistances of the cushions are:

$$R_{calc,SAMPLE01} = \frac{1}{h_{rd,cav} + h_{cv,cav}} \tag{6}$$

$$R_{calc,SAMPLE02} = \frac{1}{h_{rd,cav1} + h_{cv,cav1}} + \frac{1}{h_{rd,cav2} + h_{cv,cav2}} \tag{7}$$

where $h_{rd,cav}$ and $h_{cv,cav}$ are the radiative and convective heat transfer coefficients in the rectangular cavities, respectively. The first is calculated as:

$$h_{rd,cav} = \frac{4 \cdot \sigma \cdot T_m^4}{\frac{1}{\varepsilon_1} + \frac{1}{\varepsilon_2} - 1} \tag{8}$$

where σ is the Stefan-Boltzmann constant, T_m is the average between the two surface temperatures, ε_1 and ε_2 are the thermal emissivities of the two surfaces. As far as the convective heat transfer is concerned, it is calculated as a function of the Nusselt number (Nu) as:

$$h_{cv,cav} = Nu \cdot \frac{\lambda_{air}}{s_{cav}} \tag{9}$$

where λ_{air} is the air thermal conductivity evaluated at T_m and s_{cav} is the cavity thickness. Nu is then calculated alternatively using two correlations, therefore ending with two different values for the cavity thermal resistance. The first one is reported in (CEN EN 673, 2011) and is used as technical standard to deal with vertical cavities:

$$Nu = 0.035 \cdot (Gr \cdot \mathrm{Pr})^{0.38} \tag{10}$$

where *Gr* and *Pr* are the Grashof and Prandtl numbers respectively, calculated as:

$$Gr = \frac{g \cdot \beta \cdot \Delta T \cdot s_{cav}^3}{\nu_{air}^2} \tag{11}$$

$$\mathrm{Pr} = \frac{\nu_{air} \cdot \rho_{air} \cdot c_{p,air}}{\lambda_{air}} \tag{12}$$

with g is the gravity acceleration (9.81 m/s^2), β is the thermal expansion coefficient of air defined, ΔT is the difference between surface temperatures, ν_{air}, ρ_{air} and $c_{p,air}$ are the air cinematic viscosity, density and specific heat at constant pressure respectively, all evaluated at T_m. The second is the Ostrach correlation reported in (Incropera et al., 2007):

$$Nu = 0.22 \cdot \left(\frac{\mathrm{Pr}}{0.2 + \mathrm{Pr}} \cdot Gr \cdot \mathrm{Pr} \right)^{0.28} \left(\frac{h}{s} \right)^{-\frac{1}{4}} \tag{2}$$

where h is the height of the cavity. The validity ranges for this correlation are $Pr < 10^5$, $h/s = 2 \div 10$ and $Gr \cdot Pr = 10^3 \div 10^{10}$.

3. Results and Discussion

For both tests, the standard deviation of the boundary conditions lies in the range 0.03 °C ÷ 0.09 °C, namely within the accuracy of the globe thermometers (~ 0.15 °C). Therefore steady state conditions have been established with good accuracy across the samples. As an example of the outcomes of the tests, Figure 4 shows the surface temperature maps for SAMPLE01 obtained from the time-averaging process of the measurements.

First of all, a thermal stratification is clearly visible, with temperature rising from the bottom to the top of the sample surfaces. For SAMPLE01 on the central strip D the temperature increases by 3.2 °C on the surface towards Box 1 and by 2.9°C on the surface toward Box 2. Similar results are obtained for SAMPLE02, for which the temperature increase from bottom to top on the central strip D is 3.0°C on the Box 1 side and 3.8°C on the Box 2 side. These trends are only partially caused by the thermal layering in both chambers (along the cushion height the air temperature increases by 0.9°C in Box 1 and by 1.3°C on Box 2), while the main cause are the convective phenomena inside the sample itself. It can also be noticed that the temperature variations are mainly located toward the edges, probably due to the shape of the sample section, as it is represented in Figure 1.

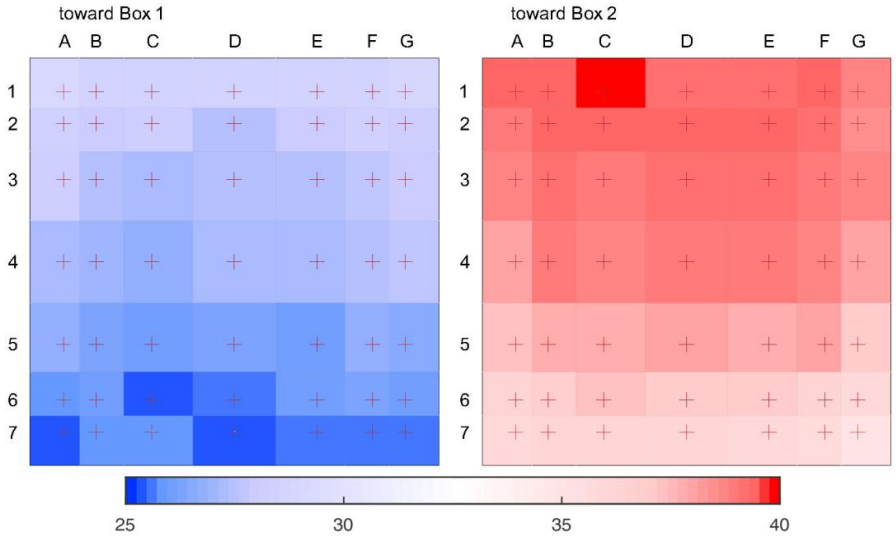

Figure 4: average surface temperature for both the surfaces (toward Box 1 and Box 2) obtained after the experimental investigation of SAMPLE01 (double layer cushion).

Table 1: average boundary conditions and weighted averages of surfaces temperatures and heat flow densities resulting from the tests performed on SAMPLE01 and SAMPLE02. Experimental thermal resistance, experimental transmittance and standard transmittance derived from tests

sample	$T_{op,1}$ **°C**	$T_{op,1}$ **°C**	ΔT_{op} **°C**	$\overline{T}_{s,1}$ **°C**	$\overline{T}_{s,2}$ **°C**	$\Delta\overline{T}_{s}$ **°C**	$\overline{\varphi}$ **W/m²**	R_{exp} **m²K/W**	U_{exp} **W/(m²K)**	U_{std} **W/(m²K)**
01	20.0	45.0	25.0	27.0	38.1	11.1	61	0.183	2.43	2.83
02	20.0	45.0	25.0	25.2	39.8	14.6	42	0.351	1.67	1.92

Table 1 shows for each cushion sample the average boundary conditions, the average surface temperatures and the average heat flow density. Under the same boundary conditions, the heat transfer through the triple layer cushion is 31% less than through the double layer one. The thermal resistance R_{exp} reported in Table 1 is equal to (0.183 ± 0.009) m^{2}K/W and (0.351 ± 0.015) m^{2}K/W for the double and the triple layer sample respectively, with expected combined errors equal to 4.8 % and 4.4 %. These results show that, even though the overall thickness of the sample is only increased slightly going from two to three layers, therefore switching from one larger to two thinner cavities, the overall thermal resistance of the cushion almost doubles (+ 91%). This might be explained by the reduction of the average thickness of the cavity that partially inhibits the convective motions, therefore reducing the heat transfer, as demonstrated also by the reduction of the average heat flux density and the rise of the average surface temperature difference. In terms of thermal transmittances (Table 1), the triple layer cushion *U*-value is about 30 % lower than the double layer *U*-value. The laboratory thermal transmittance U_{exp} is generally lower than the standard one U_{std}, indicating that convective-radiative heat

transfer coefficients in the boxes are lower than the standard ones. Indeed the purpose of the experimental measurements is mainly to compare the performances of the two cushions, rather than deriving *U*-values according to standard conditions.

By adopting air thermo-physical properties according to the thermal conditions observed during the experimental measurements and summarized in Table 1, the rectangular cavity convective-radiative thermal resistances R_{calc} have been calculated, treating the cavity thickness as a parameter. The results are reported in Figure 5 (red lines based on Ostrach correlation, blue lines based on the technical standard) and compared to the experimental results (black lines). Analysis has been performed within the range of validity and results are only taken into account when the convection is active (i.e. Nu > 1). For the triple layer sample, the cavity thickness indicated in Figure 5 refers to each of the two cavities.

By adopting air thermo-physical properties according to the thermal conditions observed during the experimental measurements and summarized in Table 1, the rectangular cavity convective-radiative thermal resistances R_{calc} have been calculated, treating the cavity thickness as a parameter. The results are reported in Figure 5 (red lines based on Ostrach correlation, blue lines based on the technical standard) and compared to the experimental results (black lines). Analysis has been performed within the range of validity and results are only taken into account when the convection is active (i.e. Nu > 1). For the triple layer sample, the cavity thickness indicated in Figure 5 refers to each of the two cavities.

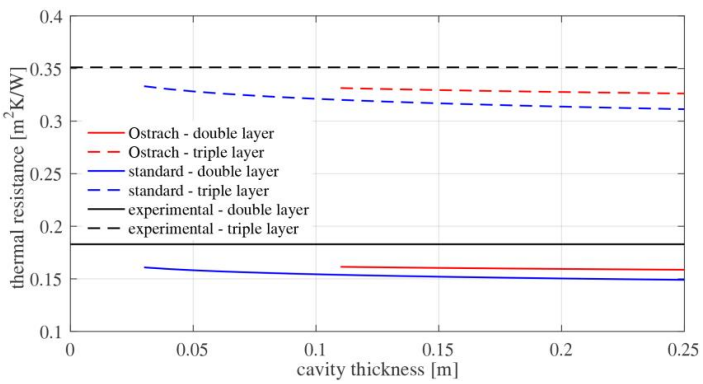

Figure 5: comparison between the experimental thermal resistances, obtained for both Box 1 and Box 2, and the results achieved using correlations from literature for vertical rectangular cavities.

As Figure 5 shows, calculated thermal resistances underestimate the measured values in both double and triple layer samples, with a slightly lower discrepancy for the thermal resistances calculated on the base of Eq. (13). If the average thickness of the double layer cushion is set to 19 cm, the calculated thermal resistance is 13-18 % less than the measured one, depending on the natural convection correlation adopted. If the average thickness of each cavity in the triple

layer sample is set to 11 cm, the calculated thermal resistance is 6-9 % less than the measured one. The discrepancy between measured and calculated values is larger than the measurement accuracy. Moreover, it can be noticed that it is not possible to find any equivalent thickness that allows to represent the heat transfer across a cushion with a vertical cavity with parallel surfaces. A possible explanation might be that the peculiar shape of the sample sections, with the tapering edges, significantly diverges from the simplified models geometry. This shape could also lead to the formation of stagnation regions inside the cushions, that might affect and reduce the overall convective phenomena, in agreement with the studies by (Antretter et al., 2008). Therefore, the next step in this work will be the assessment of this hypothesis through CFD simulations.

4. Conclusions

The main objective of this work was to compare the heat transfer performance of double layer and triple layer pneumatic cushions, by taking the effective curved geometry of the cushions into account. To this purpose, an experimental study on two small vertical samples was performed using the DAVTB apparatus, with some adaptations with respect to the original configuration in (Alongi et al. 2017). Temperature and heat flux density distributions have been mapped on both surfaces of each sample over the steady-state part of 12 h tests, and have then been used to calculate the area weighted average of the corresponding quantity. The results of this process have finally been used to calculate the overall experimental thermal resistance of the two samples, obtaining 0.183 m^2K/W and 0.351 m^2K/W for the double and the triple layer cushion respectively, with an estimated accuracy below 5 % in both cases. This shows that going from a single large cavity to two smaller ones almost doubles the overall thermal resistance of the cushion. No calculation of thermal resistance of a vertical rectangular cavity is able to effectively portray the actual behavior of the samples: both correlations analyzed tend to underestimate the experimental thermal resistances. This might be due to the unique shape of the sample cross-section, that could generate stagnation regions where the convective motions are inhibited, thus the overall insulating performance is better than what predicted by the simplified models behind the correlations.

In the future, this work will be developed on two sides: first of all, new samples will be experimentally investigated, possibly introducing textile materials provided with low emissivity coating; secondly, the convection inside the cushions will be further investigated by means of CFD simulations, in order to better understand the air motion with respect to what happens inside comparable rectangular cavities.

Acknowledgements

The authors warmly thank Prof. Alfonso Niro and Dr. Damiano Fustinoni for the FTIR spectral characterisation of the PVC coated polyester samples and of the Heat Flow Meters.

References

Afrin, S., Chilton J., Benson L. (2015) "Evaluation and Comparison of Thermal Environment of Atria Enclosed with ETFE Foil Cushion Envelope" in: *Energy Procedia*, vol. 78, p. 477-482.

Alongi A., Angelotti A., Mazzarella L. (2017), Experimental investigation of the steady state behaviour of Breathing Walls by means of a novel laboratory apparatus. In: *Building and Environment*, vol. 123, p. 415-426.

Antretter F, Haupt W, Holm A. Thermal Transfer through Membrane Cushions Analyzed by Computational Fluid Dynamics. 8th Nordic Symposium on Building Physics in the Nordic Countries 2008. Copenhagen, Lyngby, p. 347-354.

CEN EN ISO 6946 (2017), Building components and building elements. Thermal resistance and thermal transmittance. Calculation methods, CEN.

CEN EN 673 (2011), Glass in buildings. Determination of the thermal transmittance (U value). Calculation method, CEN.

Gomez-Gonzalez A., Neila J., Monjo J. (2011), Pneumatic skins in architecture. Sustainable trends in low positive pressure inflatable systems. In: *Procedia Engineering*, vol. 21, p. 125-132.

Incropera F., Dewitt D., Bergman T., Lavine A. (2007), *Fundamentals of Heat Transfer*, 6th ed, John Wiley and Sons, USA.

Interstate Standard of Russian Federation GOST 26602.1-99 (1999), Windows and doors. Methods of determination of resistance to thermal transmission.

Le Cuyer, A. (2008) *ETFE: Technology and Design*, Birkhauser.

Knippers J., Cremers J., Gabler M., Lienhard J. (2010), *Construction Manual for Polymers + Membranes*, Birkhauser, Basel, Switzerland.

Mainini A.G., Poli T., Paolini R., Zinzi M., Vercesi L. (2012), Transparent multilayer ETFE panels for building envelope: thermal transmittance evaluation and assessment of optical and solar performance decay due to soiling. In: *Energy Procedia*, vol. 48, p. 1302-1310.

Suo H., Angelotti A., Zanelli A. (2015), Thermal-physical behaviour and energy performance of air-supported membranes for sports halls: a comparison among traditional and advanced building envelopes. In: *Energy and Buildings*, vol. 109, p. 35-46.